

# Performance of a borehole heat exchanger under the influence of geothermal gradient, an exploration of BHE optimization alternatives

Hongshan Guo<sup>a</sup>, Forrest Meggers<sup>b,\*</sup>, James Tinjum<sup>1</sup>, Xiaobing Liu<sup>1</sup>

<sup>a</sup>*Andlinger Center for Energy and the Environment, Princeton University, Princeton, United States*

<sup>b</sup>*School of Architecture, Princeton University, Princeton, United States*

---

## Abstract

This paper will primarily focus on the possible consequences of considering geothermal gradient when attempting to optimize the geothermal borehole heat exchangers. Based on previous studies on the distributed thermal response test, an adaptation of an existing analytical solution of coaxial borehole heat exchanger (CBHE) is proposed. We believe it is crucial to estimate the added thermal benefit from geothermal gradient, especially when there are needs to achieve better thermal performance of the boreholes. Understanding the growing demand of geothermal energy for district systems, this paper examines the possibility of incorporating the geothermal gradient in estimating the performance of borehole heat exchangers, and subsequently the optimization of borehole heat exchanger configurations through the proposed analytical model. According to our results, the adapted analytical model was adequate to estimate the thermal responses from the test well, and can be used as a tool to estimate different coaxial borehole heat exchanger configurations. We estimate adding insulation and changing diameters of CBHEs could improve the heat extraction by up to 60% (What's the actual number?).

*Keywords:*

---

## Contents

<b>1</b>	<b>Introduction</b>	<b>2</b>
<b>2</b>	<b>Method</b>	<b>4</b>
2.1	Experiment . . . . .	4
2.1.1	Site and Borehole Heat Exchanger . . . . .	4
2.1.2	Experimental Setup . . . . .	4
2.2	Analytical Model . . . . .	6
2.2.1	Diameter, insulation level, and flow rates . . . . .	8
2.2.2	Geothermal gradient and thermal conductivity . . . . .	8
2.3	Analytical Solution . . . . .	9
2.4	Validation of adapted model . . . . .	9
<b>3</b>	<b>Results</b>	<b>10</b>
3.1	Validation Results . . . . .	10
3.2	Measurements and results from TRT . . . . .	10

---

\*Corresponding author

Email addresses: hongshan@princeton.edu (Hongshan Guo), fmeggers@princeton.edu (Forrest Meggers)

3.3	Parametric Study of other CBHE configuration . . . . .	10
3.3.1	Depth . . . . .	10
3.3.2	Insulation . . . . .	13
3.3.3	Flow rates . . . . .	16
3.3.4	Site-specific variables . . . . .	17
3.3.5	Geothermal gradient . . . . .	17
3.3.6	Soil thermal conductivity . . . . .	20
3.3.7	Performance Implications . . . . .	21
<b>4</b>	<b>Discussion and Further Optimization</b>	<b>22</b>
4.1	Room for improvement . . . . .	22
4.2	Cost implications . . . . .	24
4.3	Room for further investigations . . . . .	24

## 1. Introduction

Geothermal energy is gradually becoming a much more popular option amongst other renewable energy sources. Its abundance in near-earth surface and reliable nature during long-term operation has attracted researchers from geophysical, geotechnical and building engineering. A particular challenging task during the design of borehole heat exchangers is the estimation of desired borehole length, which is often achieved using single in-situ thermal response tests happening at or close to the site of the project. This is often achieved by averaging the thermal conductivity of the overall borehole during the entire thermal response test, which is further used in estimating the overall borehole thermal resistance, and thus ultimately the necessary length of boreholes. The most prevalent method currently used in this process was first proposed by Ingersoll in 1954. His method helped engineers to estimate the total required length of borehole heat exchanger under some common simplifications, and three hypothetical energy injection stages and assumed ground thermal resistance over time. A few fundamental assumptions of this method included homogeneous ground (temperature and geological conditions), constant heat injection rate and therefore limited emphasis on the vertical variation of heat exchange along borehole heat exchangers.

To characterise the thermal potentials of boreholes, thermal response tests (TRTs) are often used when estimating the borehole resistances. Following the ASHARE guidelines, the inlet and outlet temperature at the borehole are recorded. The thermal conductivity of the borehole is the mean rate of temperature change over the natural logarithmic time of either the inlet or outlet temperature beyond the initial period of heat injection. The thermal conductivities are further used to estimate the borehole resistance and other parameters to evaluate potential borehole field designs. This method clearly does not provide enough information regarding the temperature evolution along the depth of borehole, i.e. the geothermal gradient situation of individual boreholes.

The state-of-the-art methods used in estimating the thermal properties during thermal response tests (TRTs) were first proposed by Ingersol in 1954, and further expanded into ASHRAE guidelines in ASHRAE Handbooks. This method attempt to estimate the borehole resistance through three hypothetical stages of heat injection. The total required length of borehole heat exchangers are therefore determined through the borehole thermal resistance determined through the in-situ TRT, which is based on the assumption of the ground being completely homogenous. For district-level systems with larger heating/cooling demands, this could mean up to 4,000 boreholes (Liu, Conference proceeding 2019). As geothermal energy sources become more popular, it might be beneficial for new geothermal installations to seek alternative solutions that requires fewer boreholes due to space constraints where fewer boreholes at larger depths should ideally yield similar heat extraction/removal results.

However, the homogeneity assumption completely disregards the geothermal gradient of the ground, particularly at a larger depth. This is a temperature increase along the depth of wells at the rate of an average 25

to  $30\text{ }^{\circ}\text{C}$  per kilometer due to absorbed solar power. Under different circumstances, the geothermal gradient could vary between significantly: from as little as  $1\text{ }^{\circ}\text{C}$  to as much as  $5\text{ }^{\circ}\text{C}$ . While the ground temperature of GSHP are often considered to be around  $15\text{ }^{\circ}\text{C}$ , the temperature at the bottom of borehole could be up to  $25\text{ }^{\circ}\text{C}$  for a 500 m deep borehole heat exchanger(citation). However, as the existing thermal response tests only requires a single undisturbed ground temperature, this thermal potential may very much be overlooked since only the mean temperature of the ground is necessary for conventional TRT calculation.

Borehole heat exchangers (BHEs) used in those settings are either single U-bent or double U-bent polyethylene tube heat exchangers. The configuration of two coaxial circular tubes inserted in a borehole that is either grouted or directly driven into the soil is, comparatively speaking, much less common[1]. However, the benefit of coaxial borehole heat exchangers are more obvious when working with deeper geothermal boreholes where higher temperatures may be achieved. Using low-enthalpy deep geothermal sources have often been associated with CBHEs[2].

Specifically regarding the temperature availability, some recent studies have gone beyond treating lower temperature geothermal energy as merely a steady source of heat at a lower temperature. As the geothermal boreholes can be drilled deeper and hence producing much warmer temperature output, introducing those outputs to building systems could, therefore, lead to higher coefficients of performance (COP) or even providing for district heating[3]. Such methods include either sourcing from higher temperature geothermal basins[4] or using deeper coaxial borehole heat exchangers(CBHE) to extract copious amounts of heat from the ground [5]. Increasing the number of boreholes or increasing the borehole depths are recognised as the two directions to scale up BHE installations, as identified by Rybach et al.[6] in the 1990s. As interests in harvesting renewable energy increased, many projects in Norway and Sweden built networks of BHEs (usually shallower than 500m) [7]. Adding insulation for the inner pipe received much less attention due to the high investment necessary from the drilling and operational costs. Additionally, even accounting for the added thermal benefit in economic analysis, the results may still not justify the costs of increasing the depth of a borehole [2].

Recent research have pointed out possibilities to use distributed TRTs that utilise fibre optic sensors that produces depth-specific temperature measurement along the borehole. This approach is currently understood as the Distributed Thermal Response Test (DTRT). This approach acknowledges the temperature variations along the depth of borehole heat exchanger through the measurement of fiber optic cables, where the optic signals are interpreted as temperature distribution along the cables. This approach has been helping researchers improving their models and evaluation methods of borehole resistances (Meyer 2013) and analytical solutions (Walker 2015). A few pioneering researchers even proposed distributed thermal response test, which is essentially adding a distributed temperature sensing (DTS) cable to the borehole heat exchanger during the investigation. However, while most of these investigations were successful, the driving force of the differences between heat fluxes at different depths remains to be further understood: the heterogeneity of the ground is still oversimplified within the existing DTRT methods, particularly with respect to the different underground water flow and thermal properties of different ground layers.

This paper aims at changing this status-quo by adapting an existing analytical solution of coaxial borehole heat exchanger under the influence of geothermal gradient. We will validate the adapted model through the experimental data collected during a recent test well drilled on campus at Princeton University, which provide further validation for the model's usage in predicting the thermal responses of borehole heat exchangers under the influence of geothermal gradient. We also aim at generating the potential changes in performance when alternative designs of coaxial borehole heat exchangers' (CBHEs) configurations and insulation levels are considered. We hope this paper is the first of many to set the ground for future comparison with DTRT methods used and designed for coaxial borehole heat exchangers proposed by McDaniel.

The primary goal of this paper is to estimate the potential performance improvement through changing the configuration

## 2. Method

### 2.1. Experiment

#### 2.1.1. Site and Borehole Heat Exchanger

Need for geothermal district heating/cooling demand for potentially the entire campus. It is crucial to assess the possibilities of using deeper geothermal heat exchangers.

The drilling of the well took place beginning August 8th, 2019. To characterize the formation layering at the drill site, a geological survey was performed immediately after the drilling. On top of the drilling of the site identified began on August 12th, 2019, and encountered significant amount of underground water upon reaching approximately 150 feet (45.7 meters) depth. The composition of the ground was primarily sand stone and mudstone until hitting gravel at approximately 1000 feet (300 meters) depth. The remainder of the drilling to approximately 1400 feet (430 meters) took significantly longer, and appeared to have hit quartz and hence halted the drilling of the test bore at 1440 feet the subsequent day. USGS (United States Geological Survey) performed a geophysics survey on the test bore immediately after the drillers pulled out, and determined similar geological make up of the test bore, and determined the actual length of the borehole to be approximately 1340 feet (410 meters). The hydro-geological conditions of the drill site is shown in Figure 1.

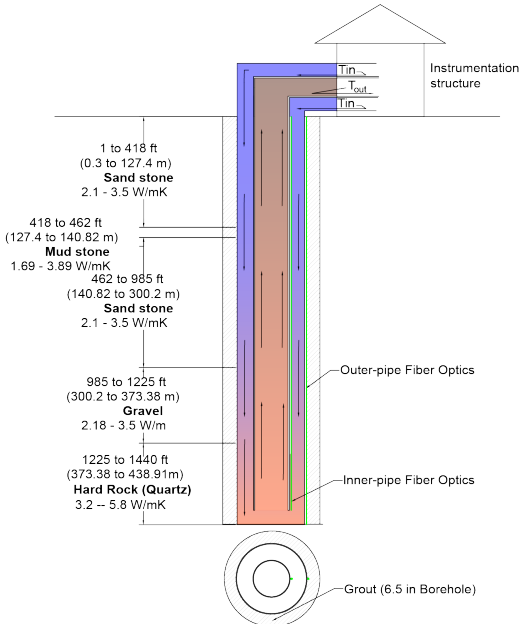


Figure 1: Hydro-geological condition estimated through USGS survey immediately taken after the drilling of the well estimated at 1440 ft(438.9 m).

As is shown in Figure 1, the geological conditions around the borehole varies significantly inside the BHE. This phenomenon is not very well-represented in conventional thermal response tests.

#### 2.1.2. Experimental Setup

To characterise the thermal potentials of boreholes, thermal response tests (TRTs) are often used when estimating the borehole resistances. Following the ASHARE guidelines, the inlet and outlet temperature at the borehole are recorded. The thermal conductivity of the borehole is the mean rate of temperature

change over the natural logarithmic time of either the inlet or outlet temperature beyond the initial period of heat injection. The thermal conductivities are further used to estimate the borehole resistance and other parameters to evaluate potential borehole field designs. This method clearly does not provide enough information regarding the temperature evolution along the depth of borehole, i.e. the geothermal gradient situation of individual boreholes. Recent research have pointed out possibilities to use distributed TRTs that utilise fibre optic sensors that produces depth-specific temperature measurement along the borehole.

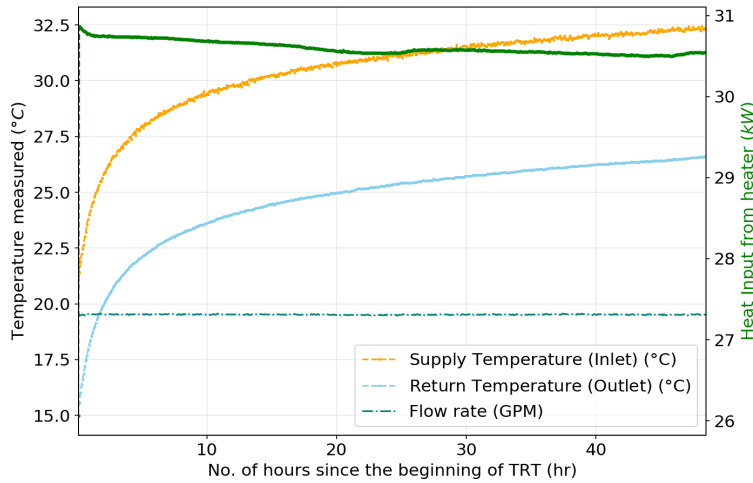


Figure 2: Temperature measured at the inlet and outlet of the well site during the thermal response test.

As we have previously suggested in the introduction, we are particularly interested in the effect of geothermal gradient in this study, for which we would be more interested in using coaxial borehole heat exchangers over conventional U-tube borehole heat exchangers. The CBHE option the test well project was able to procure is a Rygan borehole heat exchanger. Upon finishing the drilling and USGS geological survey, the outer pipe of the CBHE is first inserted into the test bore before it was grouted. The grout was left to set for over 24 hours until the next step of heat exchanger installation. A Rygan concentric heat exchanger was then installed into the drilled test bore, and grouted with a GeoPro TG select/PowerTEC 1.6, whose target thermal conductivity was 0.78W/m-K at a density of 1.2kg/L. The borehole heat exchanger has a diameter of 6.5 inch (16.5 cm) from 380 to 1340 feet. The inner diameter of the CBHE, or the OD (outer diameter) of the Rygan tube was a 2.66 inch (6.76 cm?) and corrugated. Although this will obviously change the fluid dynamics of the flow in the annulus, we will assume the outer surface of the Rygan heat exchanger (inner tube of CBHE, not to be confused with CBHE outer tube) to be smooth within the scope of this research.

To estimate the thermal conductivity of the formation, a thermal response test was performed on the drill site on September 10th, 2019. The test follows the guidelines recommended by the American Society of Heating, Refrigeration and Air-Conditioning Engineers (ASHRAE) in its HVAC Applications Handbook, Geothermal Energy Chapter. The borehole was uniformly grouted from the bottom to the top via premix pipe, and had a delay of more than five days between loop installation and test startup. The undisturbed formation temperature was estimated through the recorded temperature from the fiber optic cable installed along and around the borehole heat exchanger. The duration of the test was 48.5 hours, where the data (inlet, outlet temperature and heat injection rates) was collected every five minutes. The heat injected was estimated to be 51 to 85 Btu/hr (or 15 to 25 W) per foot of the borehole, which averaged to be approximately 30.5 kW total heat input throughout the test. By taking the natural log time rate of change of the temperature of either the inlet and the outlet, and can be further expanded into the thermal diffusivity of the formation through an estimated heat capacity of the borehole. The estimated heat capacity of the

bore can be estimated through the geological conditions previously confirmed through drilling (as shown in Figure 1).

We positioned two fiber optics cable along the outer surface of both the inner and the outer pipe of the CBHE, i.e. the corrugated outer surface of the Rygan heat exchanger, and the CBHE outer tube. Fiber optic distributed temperature sensing has been previously used by many researchers to perform measurement on the therm-physical properties around boreholes in previous research(Fujii et al. 2009, Beier 2012, Acuna 2013). This is a technique that utilize the optic power measured through silica core in fiber optic cables, applying time-domain reflectometry principles and output temperatures at discrete locations adjacent to the fiber itself. Previous studies have shown the benefits of employing DTS in TRT testings, and even pointed to enhanced versions of TRT (known as DTTRT) and were able to interpolate the DTS readings into depth-specific thermal conductivities(McDaniel). We installed a similar setup during our experiment, using two type-T (copper/constantan) thermocouple was attached to the data logger to monitor the reference temperature used to calibrate the readings coming in through the data logger. We used an Oryx interrogator (Sensornet, London, UK) to interpolate the data from the fiber optic cable. As the interrogator provided temperature resolution as fine as 0.01 C, and a spatial resolution as fine as 1m, we opted for various sample interval during the TRT test. During the first 10 hours of the test, we used 1 minute intervals, which was extended to 2 minutes for the subsequent measurements, including the decay test.

The overall borehole resistance  $R_b$  may therefore be estimated through Equation 1[8]. The resulting temperature profile that may lead to the improvement of the temperature can therefore be

$$R_b = \frac{H}{Q} \left\{ T(t) - T_g - \frac{Q}{4\pi\lambda_g H} [E_i(\frac{r_b}{4\alpha_g t})] \right\} \quad (1)$$

However, there are some inherent limitations of this method. First and foremost is the homogeneity assumption of the ground. The conventional method clearly assumes the ground to be at a homogeneous temperature along the depth of the heat exchanger, where the thermal conductivity, thermal diffusivity are also constants. However, as can be observed from Figure 1 produced from the USGS measurement, it was clearly not the case. In particular, the hard rock or quartz at the bottom of the borehole will likely lead to a much larger thermal conductivity of the borehole, allowing the working fluid to extract more heat at the same flow rate. Within the scope of this paper, we will continue to use a single thermal conductivity calculated from the thermal response test (and the time log temperature gradient thereof) at the top of the heat exchanger to continue our analysis. However, for future research, it is desirable to expand this into a more detailed DTTRT study.

## 2.2. Analytical Model

We will be adapting the analytical model from Beier et al., which was developed to predict the thermal response from a CBHE with known geological parameters. This model was developed to adopt undisturbed ground temperature measurement from fiber optic temperature sensors (also referred to as distributed temperature sensor, or DTS).

Typically, the overall thermal resistance of a geothermal bore can be considered as the combined resistance of the bore and the ground. The bore thermal resistance can be affected by many parameters, including the pipe material, configuration of the heat exchanger as well as the thermal conductivity of the grout/backfill in the bore annulus. The ground resistance is dependent primarily on the thermal conductivity and the diffusivity of the surrounding formation. For a vertical BHE, its thermal resistance is the combined effect of pipe resistance and bore annulus grout resistance. As Kavanaugh and Rafferty pointed out, the terms of pipe and grout resistance can be combined into a single Equation 1.

$$R_b = R_p + R_{grt} = R_{film} + R_{tube} + R_{grt} = \frac{1}{\pi d_i h_{conv}} \frac{\ln(d_o/d_i)}{2\pi k_p} + \frac{\ln(d_b/d_o)}{2\pi k_{grt}} \quad (2)$$

This equation translates the thermal resistance of the pipe to the combination of the pipe resistances and the fluid film resistance inside the pipe wall. For coaxial borehole heat exchanger, this translates to both the film resistance at the inner pipe and the borehole wall, as well as the tube thermal resistance of both the outer and inner pipes. Calculation of the tube thermal resistance is relatively straight forward as the values required includes the diameter of the tubes and the thermal conductivity of it. However, as we are more interested in varying the configuration and insulation level at the borehole as we are showing conceptually in the section of the CBHE, we need to expand the existing definition of the shunt resistance of the borehole heat exchanger. Building on the existing expressions from Kavanaugh and Rafferty (2014) as well as Beier et al. (2012), we have a new expression of the shunt resistance of the borehole  $R_{12}$ .

More specifically, the shunt resistance  $R_p$ , or sometimes referred to as  $R_{12}$  of the CBHE is a parameter that we can modify to achieve different yield from a known location with certain geological condition. From the schematic diagram, it is evident that any design intervention to change the performance of a CBHE needs to happen at the level that affect the shunt resistance. This expression allows us to evaluate the thermal resistances of CBHEs, we group the contributing variables into two categories: direct and indirect. Direct variables are the diameters of the inner and outer pipes, thermal conductivity of the pipe material, and the thickness and material of the insulation material inside the inner pipe. The flow rate entering the CBHE is the indirect variable, which not only affect the convective heat transfer coefficients contributing to the film thermal resistances. To provide a more accurate description of the thermal resistance of the shunt resistance, expression of  $R_{12}$  needs to be updated as Equation 3. This includes the film thermal resistances at the heat exchanger surfaces, and the thermal resistances that represents the conductive heat transfer through the pipe and insulation materials, i.e.  $R_{pw1}, R_{ins}, R_{pw2}$ . More explicitly, these individual expressions can be written as Equation 5, where the overall shunt resistance may change with respect to different CBHE configurations. This is also expressed in Figure 3.

$$R_{12} = R_{fi} + R_{pw1} + R_{ins} + R_{pw2} + R_{fo} \quad (3)$$

$$Nu = \frac{hL}{k} \quad (4)$$

$$\left\{ \begin{array}{l} R_{fi} = \frac{1}{\pi d_{pi} h_{pi}} \\ R_{pw1} = \frac{\ln(\frac{d_{pw1}}{d_{pi}})}{2\pi k_{pw}} \\ R_{ins} = \frac{\ln(\frac{d_{pw2}}{d_{pw1}})}{2\pi k_{ins}} \\ R_{pw2} = \frac{\ln(\frac{d_{po}}{d_{pw2}})}{2\pi k_{pw}} \\ R_{fo} = \frac{1}{\pi d_{po} h_{po}} \end{array} \right. \quad (5)$$

If we may overtly simplify the entangled the relationship between the depth, performance and cost can be generalised into a statement: the further down the reach of the borehole, the higher the bottom of borehole temperature, and the larger the drilling costs and operational (pumping costs). And to improve the heat exchanger capability of any CBHE, we will therefore need to either change the configuration of the CBHE, or the location of the CBHE. This can be categorized into either shunt-resistance-related parameters and the site-specific parameters.

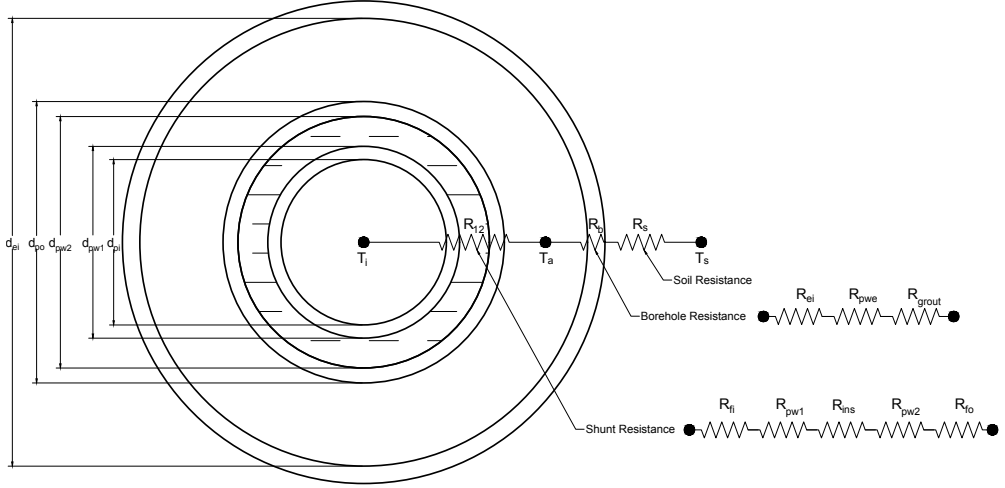


Figure 3: Schematic diagram of thermal resistance calculation for borehole.

#### 2.2.1. Diameter, insulation level, and flow rates

Diameters, insulation level and flow rates are parameters that we may subjectively alter to modify the performance of borehole heat exchangers. To better utilise the geothermal energy that is returned to the ground surface, insulating the inner pipe of CBHEs so that the heat transfer between the inner tube and annulus will not short-circuit the heat extraction in the CBHE. The resulting importance of adding insulation on the inner pipe was highlighted in a few previous publications [9, 10] but was found to be not economically feasible for project proposal[2]. One such study came from Dijkshoorn et al. , in which the construction and measurement of a 2500m deep well helped to validate the modelling of satisfying borehole performance over 30 years when using the borehole output to drive a climate control adsorption chiller. However, their results did not support the extra investment of adding an insulated inner pipe for the borehole - the entire project came to a halt at such. Additionally, despite acknowledging the possibility of added thermal benefit by inserting an insulated inner pipe, this was not further pursued due to cost constraints. In a very recent publication, the effect of changing the pipe configuration to achieve better thermal performances, but does not vary the design and environmental (specifically on the geothermal gradient) parameters component-by-component in CBHE design[11].

#### 2.2.2. Geothermal gradient and thermal conductivity

Using the same set of method outlined by Beier et al. [8], it is possible to use an arbitrary temperature profile as the undisturbed ground temperature and solve for corresponding ground temperature.

Another modification of the method we're adapting is described as Equation 6, where the temperature distribution along the depth of CBHE can be considered constant at locations that are infinitely far away from the center of the test well.

$$\frac{\partial T_{DS}}{\partial z_D}(r_D \rightarrow \infty, t_D, z_D) = g_D(z_D) \quad t_D > 0 \quad (6)$$

Geothermal gradient, thermal conductivity, are parameters that varies objectively, but varies significantly enough spatially that could also affect the performance of a CBHE. Addressing the presence of geothermal gradient is therefore extremely important when the proposed boreholes are deeper rather than shallower. Existing studies show that geothermal gradient may vary between 1 to 5 Kelvin per hundred meters' depth[7, 12].

### 2.3. Analytical Solution

For each time step, a new analytical solution can be solved along different  $t$ ,  $r$  and depth in CBHE. Following the same set of method

As we are interested in the possible benefits of designing CBHEs better through different combinations of configurations, we are primarily interested in creating a lightweight algorithm that allows us to compare the expected thermal response outcomes (particularly the thermal resistances or heat extracted) between the different configurations. We therefore adapted the analytical method from Beier et al. [13] with the following modifications: expanded the shunt resistance expression to allow for extra thermal insulation inside the inner pipe; adopted geothermal gradient into the undisturbed ground temperature during the solving of the target temperature function and translated the original analytical model from MathCAD into Python as a class that allows parallel comparison of the resulting thermal resistance of the boreholes.

Therefore, for every time step during a simulated hypothetical time step, the corresponding analytical solution can be calculated for a given radius, depth and time since operation. Using Laplace transformation, the heat exchange within the central and annular flow can be solved using the Navier-Stokes equation with boundary and initial conditions. As all the variables were converted into dimensionless form, including the time component, the analytical solution requires an inverse Laplace transform to calculate temperatures in the time domain. The detailed solution of the energy equations using the initial and boundary conditions can be found in the appendix for the annulus as inlet scenario. We used the Stehfest algorithm following Beier's example in his 2013 paper[14] to perform the inverse laplace transformation.

### 2.4. Validation of adapted model

To confirm the validity of our adapted model, we want to compare the temperature profile that we can create by modeling the temperature distribution inside the CBHE. The parameter we used as the model input are as the followings shown in Table 1.

Parameter	Symbol	Value
Borehole radius	$r_b$	115 mm
Active heat exchanger length	L	170 m
Inner pipe outer radius	$r_{po}$	40 mm
External pipe outer radius	$r_{eo}$	114 mm
Inner pipe thickness	$d_{pp}$	2.4 mm
External pipe thickness	$d_{ep}$	0.4 mm
Inner and external pipe wall thermal conductivity	$k_{pp}, k_{ep}$	0.40 W/(K·m)
Ground thermal conductivity	$k_s$	3.15 W/(K·m)
Ground volumetric heat capacity	$c_s$	$2.24 \times 10^6$ J/(K·m <sup>3</sup> )
Water flow rate	w	$0.58 \times 10^{-3}$ m <sup>3</sup> /s
Water density (at 15°C)	$\rho$	999 kg/m <sup>3</sup>
Water volumetric heat capacity (at 15°C)	$c_w$	$4.19 \times 10^6$ J/(K·m <sup>3</sup> )
Water thermal conductivity (at 15°C)	$k_w$	0.59 W/(K·m)
Water dynamic viscosity (at 15°C)	$\mu_w$	$1.138 \times 10^{-3}$ kg/(m·s)
Reference soil surface temperature	$T_{rs}$	8.9°C
Nondimensional temperature of soil	$T_{DS}$	
Nondimensional temperature of inlet/outlet	$T_{D1}, T_{D2}$	

Table 1: Nomenclature, input parameters used in determining the performance of CBHE.

### 3. Results

#### 3.1. Validation Results

Using the parameters set out in Table 1 and the model we adapted, we were able to compare the temperature of our simulation against the temperature profile measured inside the CBHE during the TRT process.

#### 3.2. Measurements and results from TRT

We were able to determine the corresponding thermal conductivity through the conventional TRT results. The undisturbed ground temperature

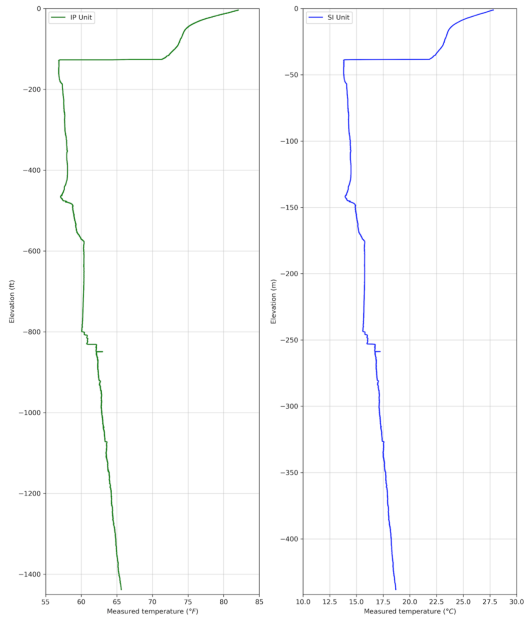


Figure 4: Temperature measurement from fiber optic cable attached to the outside of CBHE at test site prior to the commencement of TRT.

#### 3.3. Parametric Study of other CBHE configuration

We're interested in improving the thermal performance of the borehole heat exchanger, particularly with respect to the designed and site-specific variables.

##### 3.3.1. Depth

The largest motivation of this study was to investigate the influence of geothermal gradient on CBHE performance, and what that might mean when considering a CBHE design. The total length of the BHEs are conventionally determined through the guidelines set by ASHRAE Handbook [15], which was originally proposed by Ingersoll and Zobel [16] and further adjusted by Kavanaugh [17]. This method requires the thermal conductivity, diffusivity of the soil as well as the borehole thermal resistance per unit length, establishing a clear link between the depth of the CBHE with the resulting heat extraction rate variation along the borehole, but with no geothermal gradient assigned to the model, added depths only increases heat exchange area and not the reference ground temperature.

Geothermal gradients are commonly known to be within 25 to 30 Kelvins per kilometer for shallower layers of ground [7]. We therefore assume a geothermal gradient of 30 K per kilometer for this analysis where different depths could be used in designing a CBHE[12]. This is to be expected to be representative of an average condition for deeper geothermal boreholes. For the undisturbed ground temperature profile, we used the measured data from Beier's research for the first 178 meters, and extrapolated the rest of the borehole length with the geothermal gradient we selected. We also held the rest of the borehole configuration constant, following the Beier study from 2013, changing only the depth of a borehole to achieve different vertical temperature profiles. To avoid the more transient first few hours, only the vertical temperature profiles at the 100th hour will be compared against one another. To better illustrate how this may affect the heat extraction rate, we will also be using a second set of legend to show the heat extracted averaged by length in  $W/m$  from the borehole via Equation 7. The results we will be showing in the vertical temperature profiles will be the 100th hour condition, and will remain so unless otherwise specified in the legend and caption.

$$q_{out} = c_w \dot{m} \frac{T_{out} - T_{in}}{L} \quad (7)$$

We picked five borehole lengths at 50 m, 150 m, towards the deeper ones at 500 m , 1000 m, 1500m and 2000 m as an extreme to examine the temperature distribution vertically with the original horizontal borehole configuration as shown in Beier's research [14]. We examined both the comparison plot with the actual and dimensionless depth as the y-axis to determine the more legible option. It is expected that the base case will have much of the thermal energy available at the bottom of borehole taken away due to a smaller shunt resistance. Increasing the shunt resistance could theoretically improve the thermal performance of the boreholes.

Intuitively, a good design intervention to increase the thermal performance of CBHE is to insulate the inner pipe. To demonstrate how insulation alone could change the thermal performance of a CBHE, we also examined an ideal case where we assume the insulation material that we calculate  $R_{ins}$  from is vacuum. We do so by assuming CBHE has vacuumed space as the insulating material, resulting in a thermal conductivity of  $k_{pp} = 0.007W/(m \cdot K)$  across the shunt and thus, giving a best case scenario of the temperature profile and heat extraction rate. It is important to point out the vacuum case is merely an ideal and hypothetical scenario instead of a realistic one. Even with a somehow vacuumed insulating inner paper, it is highly unlikely that the vacuum can be maintained during prolonged CBHE operation, i.e. can be used for actual implementation for a CBHE. The vacuum scenario is, at its best, an ideal condition that illustrates the best operating scenario with a super-insulated central pipe, or how helpful insulation could be in when designing CBHE operating with a larger bottom of borehole temperature. It should be noted that this is highly unlikely to be achievable by actual CBHEs, since not only will there be additional engineering challenges in addressing the decreased average density of the shunt, there will also need to be separate analysis on how to properly insulate a CBHE to maintain its long-term insulated performance, all assuming that the added cost of insulating the inner pipe can be justified.

We obtained the vertical temperature distribution as shown in Figure 5. We obtained the vertical temperature distribution as shown in Figure 5. As expected, the presence of geothermal gradient leads to increased heat extraction rate for deeper boreholes. The heat extraction rate, however, does not increase proportionally with the depth increase, as the amount of heat extracted only increased by approximately 12.6% when the assumed CBHE length increases from 1000 m to 2000 m. The amount of extra investment to both drill the borehole and the additional cost of in casing to avoid borehole collapsing could also be significant. Between the six depths tested, it appears that a preferred length of CBHE could be 1000m, since the heat extraction rate exhibit the most significant jump for the first kilometre only for a CBHE whose far-field temperature distribution is driven by geothermal gradient at 3 Kelvin every 100 meters only. The length of a CBHE is therefore set to be at 1000 m for the remainder of this study. An interesting trend for temperature evolution along the discharge pathway is that the inlet and outlet appeared coupled, while the heat exchange between the inlet and outlet pathways works against the purpose of heat extraction.

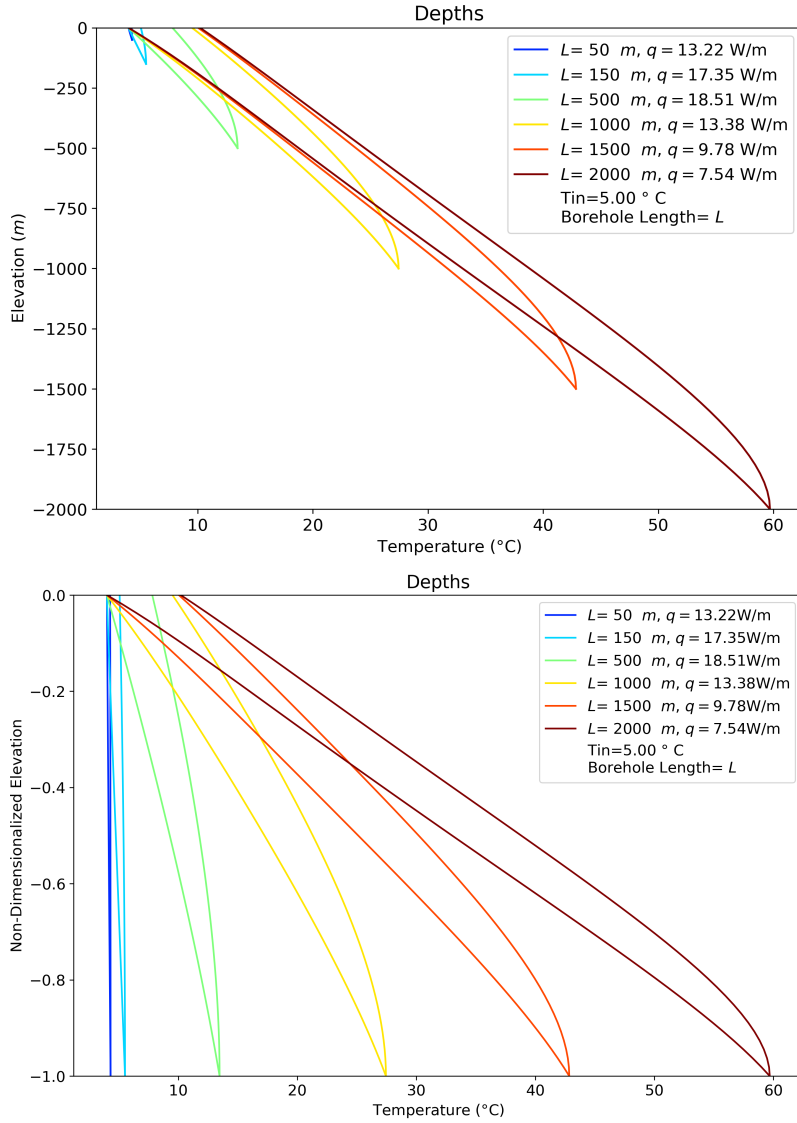


Figure 5: Actual vertical temperature distribution of CBHE with length of 50, 150, 500, 1000, 1500, 2000 m with actual depths (left) and dimensionless depths (right).

To best avoid the heat transfer between the two pathways, i.e. using an artificial scenario where the inner pipe is vacuumed to achieve a thermal conductivity of vacuum where  $k_{pp} = 0.007 \text{ W}/(\text{m} \cdot \text{K})$ , the temperature distribution and heat extraction rate shown in Figure 5 becomes Figure 6. The heat extraction rate drastically increases, despite the thermal conductivity being hypothetical and potentially challenging to reach for a real CBHE as the inner piping can easily float out from the CBHE well driven by its buoyancy. Most materials become succumb to the hurdle where the smaller the thermal conductivity, the lower the material density. Alternatively, an inner pipe that is double-layered and vacuumed in between could also help achieve the best insulation, yet not only will the manufacturing be challenging, there's also an explicit economic constraint for a deeper CBHE. It is therefore essential to seek alternative methods to achieve maximised heat extraction rate, or more specifically, whether it might be possible to achieve comparable if not better heat extraction rate by making incremental changes to a CBHE design.

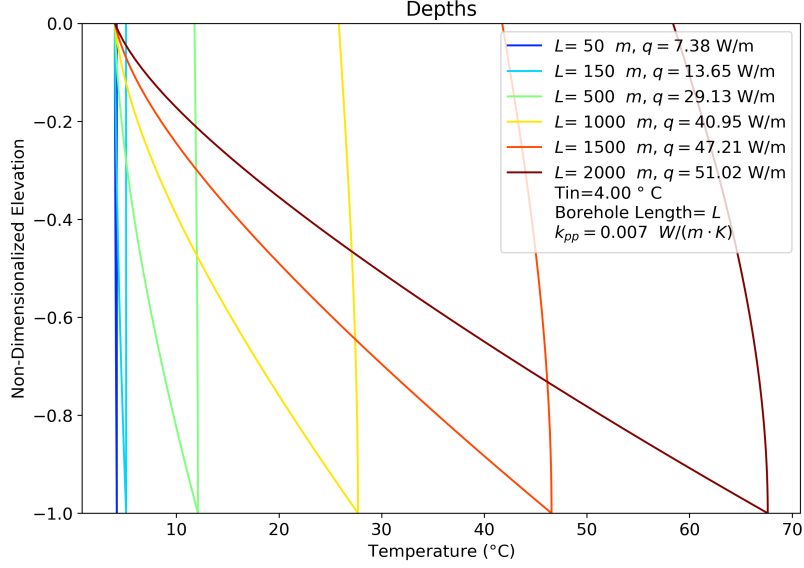


Figure 6: Vertical temperature distribution of CBHE with length of 50, 150, 500, 1000, 1500, 2000 m with non-dimensionalized depth with added assumed insulation of  $k_s = 0.007W/(m \cdot K)$ .

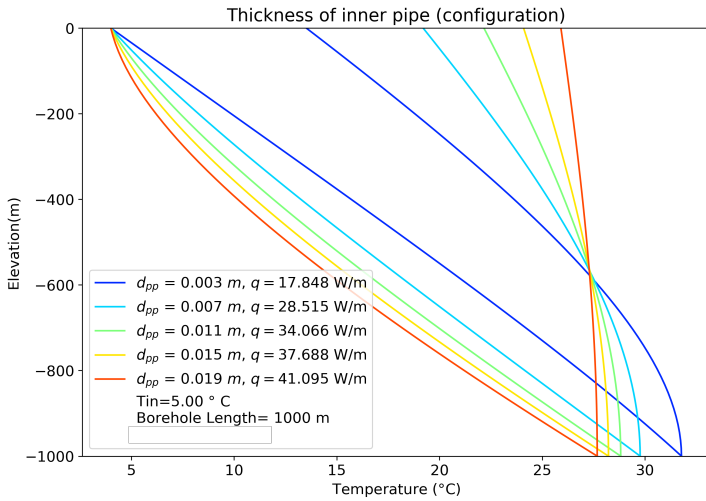
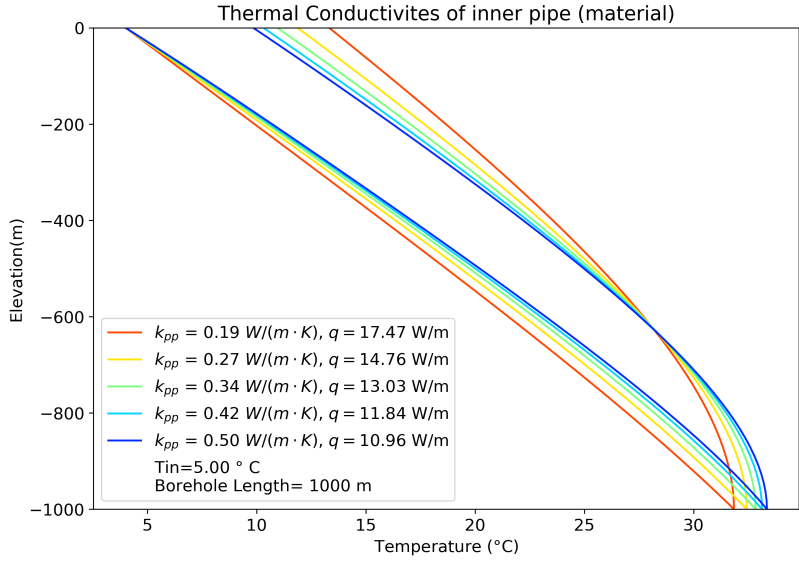
### 3.3.2. Insulation

As was mentioned above, adding insulation to the inner wall of a CBHE appears to be an ideal solution to ensure maximized heat extraction at a larger depth. To reduce the material and construction cost of a CBHE, a natural question to ask is whether decreasing the thermal conductivity of the inner pipe and increasing its thickness could lead to improved overall heat and temperature extraction. This is analyzed by assuming the borehole length is 1000 meters, which appears to be a relatively good depth to observe the influence of geothermal gradient according to our previous results obtained on the depths analysis.

For thermal conductivities of the inner pipe, the commercially available PP piping has a  $k_{pp}$  ranging from 0.19 to 0.5  $W/(m \cdot K)$  for PP piping and results in apparent changes of vertical temperature profiles and heat extraction rate as is shown in Figure 4. The smallest thermal conductivity of the material used was 0.19  $W/(m \cdot K)$ , resulting in a larger shunt resistance  $R_{12}$  and hence a better heat extraction rate. With the thermal conductivity increasing to 0.5  $W/(m \cdot K)$ , the heat exchange between the central and annular flow gradually increases, causing a gradual increase of the short-circuiting of the CBHE - the flow travelling upward loses more heat to the inner pipe as it travels to near ground-surface.

We then further modified the CBHE configuration by varying the thickness of the inner pipe wall, such that the shunt thermal resistance also increases such that the heat exchange between the inlet and outlet can be decreased further. Varying the thickness of the inner pipe and holding the inner pipe diameter constant, the actual cross-section area of the inner pipe (AD1) reduces as the area ratio  $r_{12}$  increasing, and we were able to obtain Figure 8. Increasing the thickness of the inner pipe from 3 mm to 19 mm changes the vertical temperature distribution inside the CBHE at the 100th hour. Altering the thickness of the inner pipe appears to have effectively increased the heat extraction rate and minimised the heat transfer through the shunt, leading to a much-improved temperature decrease along the central pipe for the flow upward.

The resulting heat extraction rate with the most substantial thickness exceeds the heat extraction rate obtained in the fictional thermal conductivity assumed in Figure 6 for the 1000 m deep CBHE at 41.095  $W/m$  at the 100th hour of the simulation. A natural question then arises on whether it would also make sense for the outer pipe when its thermal resistance is minimised, could have improved the thermal performance of CBHE at a similar order of magnitude. To do so, we first examine the results of varying the thermal



conductivity of the outer pipe in Figure 9. It does not appear to have as significant an effect on the resulting temperature distribution at the 100th hour as shown in Figure 9.

To better examine the result of varying the outer wall thickness and the resulting temperature profiles, we analysed different  $k_{ep}$  from  $0.5 \text{ W}/(\text{m} \cdot \text{K})$ , as well as  $k_{pp}$  at  $0.19 \text{ W}/(\text{m} \cdot \text{K})$ , which led to results shown in Figure 10. The thicker the outer pipe, the slower the heat extraction along the annulus, and the smaller amount of heat extraction rate at the inlet/outlet of the borehole, as can be observed from Figure 10. It is vital, therefore, to keep the thermal conductivity for the outer pipe as large as possible, while maintaining

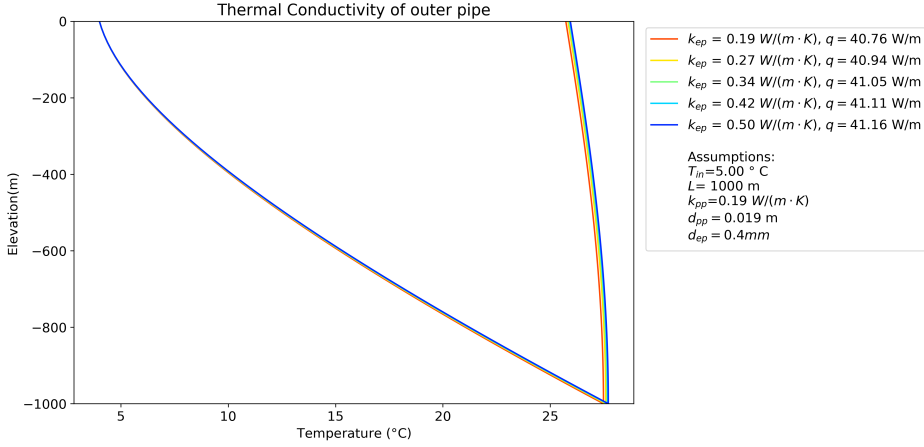


Figure 9: Vertical temperature distribution profiles resulting from variation of thermal conductivity of the outer pipe at the 100th hour of simulation.

the thickness of the outer tube as small as possible. Hence the thermal conductivities of the inner and outer pipe becomes  $k_{pp} = 0.19W/(m \cdot K)$ ,  $k_{ep} = 0.50W/(m \cdot K)$ , while the thickness of the inner and outer pipe becomes  $d_{pp} = 0.019m$ ,  $d_{ep} = 0.0004m$ . We selected  $d_{ep}$  following the Beier publication as an identified thinnest outer pipe CBHE.

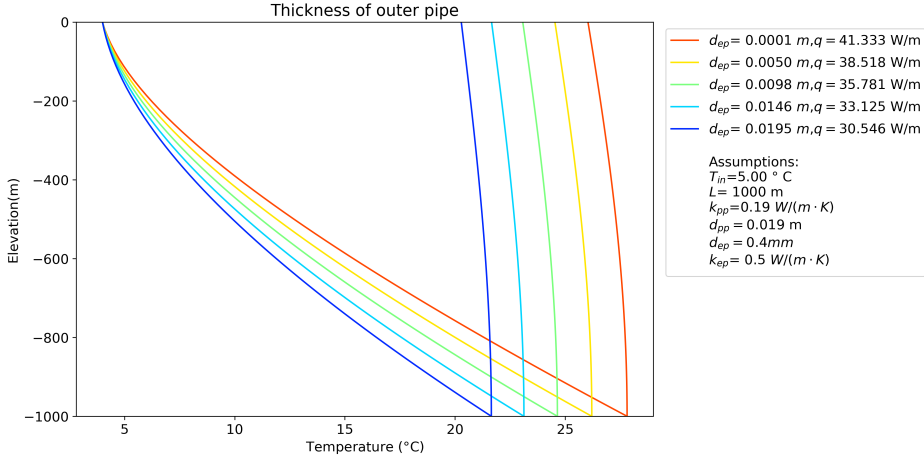


Figure 10: Vertical temperature distribution profiles resulting from variation of thickness of the outer pipe at the 100th hour of simulation.

Additionally, these results could suggest improved performance inside standing column wells when they are deep and come into contact with the warmer ground due to the geothermal gradient. Without having a thermally conductive grout, a standing column well may have a considerably better performance when the wells are deeper with larger surfaces for heat exchange. The primary challenge for modelling standing column wells might be the added friction from not having smoother PVC pipes as flow channels, resulting in difficulties both in terms of modelling as well as operational cost increase.

### 3.3.3. Flow rates

Varying the flow rate inside the CBHE will also naturally lead to variations of the vertical temperature profiles. Hence we compared the configuration selected so far with a specific set of flow rates, ranging from laminar flow to turbulent flow, from  $0.0001$  to  $0.005 m^3/s$ , as shown in Figure 12. As the flow rate increases, the heat extraction rate also increases. Observing the vertical temperature distribution variation over time under different flow rates, as shown in Figure 11, the temperature profiles coloured concerning how far along the simulation went, with the initial conditions marked as blue, and the last states marked out as dark red/brown.

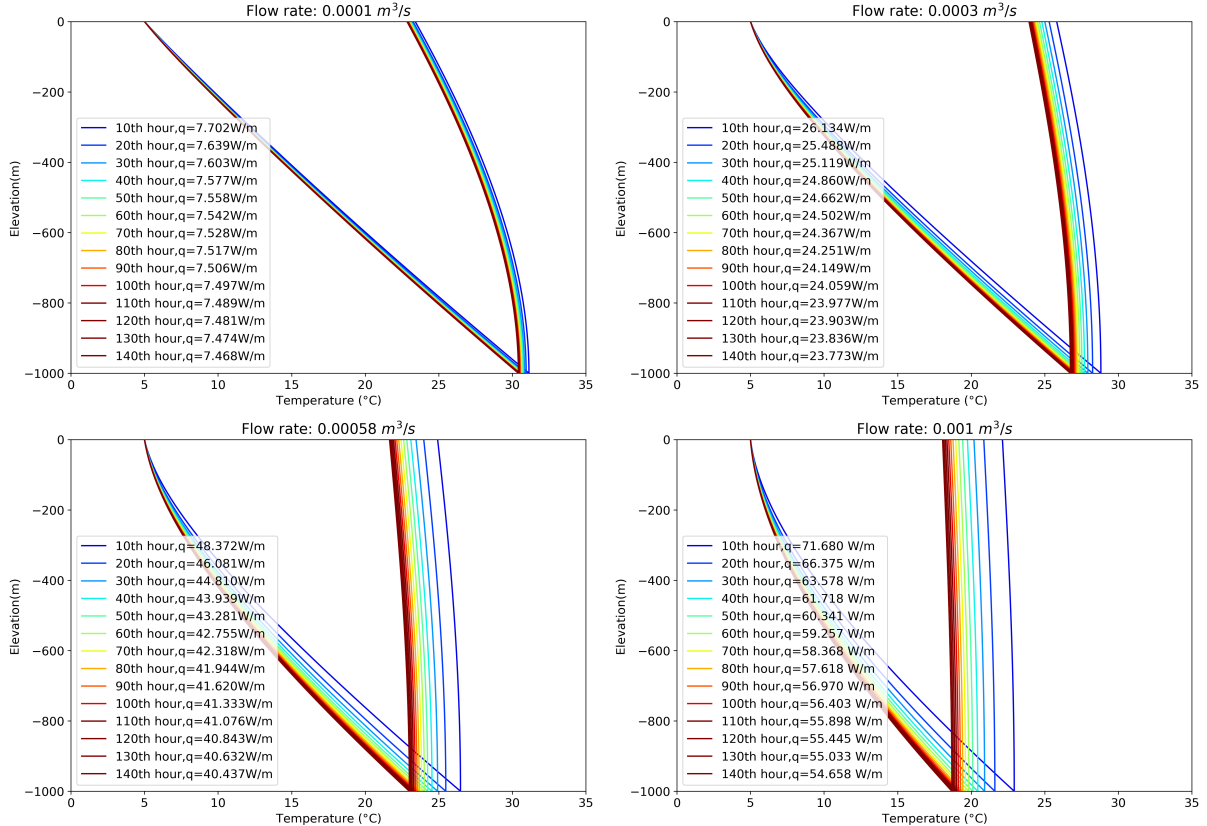


Figure 11: Vertical temperature distribution and its variation over time for different flow rates:  $w = 0.0001 m^3/s$  (top left),  $w = 0.0003 m^3/s$  (top right),  $w = 0.00058 m^3/s$  (bottom left),  $w = 0.001 m^3/s$  (bottom right).

To better illustrate how the heat extraction rate changes over time, we plotted the heat extraction rate of the 1st 1000 hours as shown in Figure 10. As all the heat extraction rate gradually falls lower, the model yields a relatively steady heat extraction rate for all six flow rates. The increase from the flow rate of  $0.00058 m^3/s$  to  $0.001 m^3/s$  results in a limited increase of heat extraction rate of less 5%. Since increasing the flow rate will also increase the pumping cost for the operation, this small increase of heat extraction rate does not easily justify the increased operational costs. A more desirable flow rate is, therefore, set at  $0.001 m^3/s$  to achieve better heat extraction rate, but at a smaller flow rate and therefore smaller necessary pumping power for further analysis. The temperature out for this remains steady at approximately  $18.5 ^\circ C$ , which could be desirable for a high-COP GSHP, but not suitable yet for direct heating.

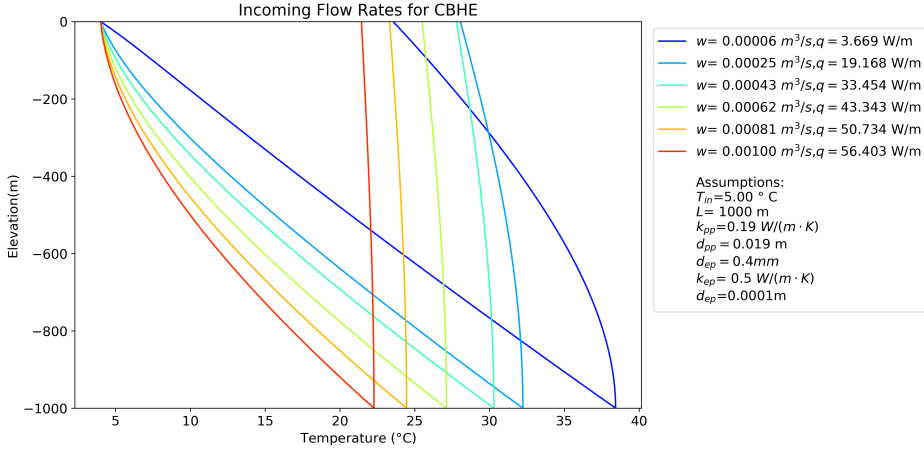


Figure 12: Vertical temperature distribution and heat extraction rate at 100th hour

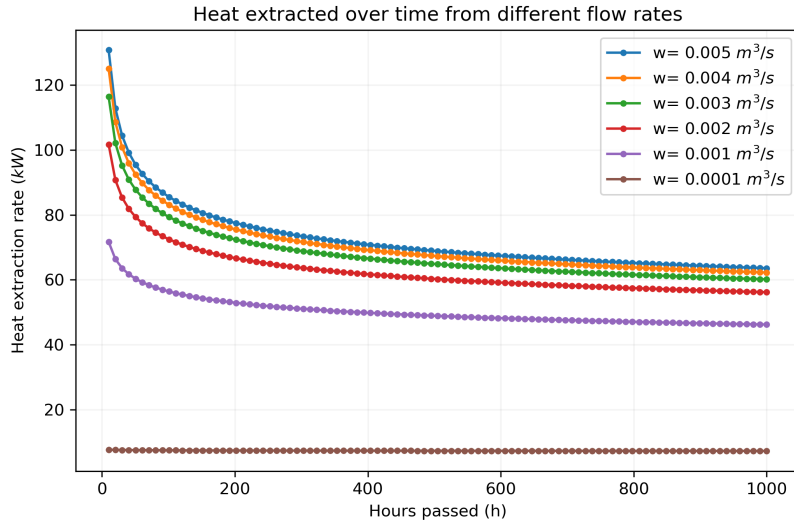


Figure 13: Heat extraction rate variation over 1000 hours for different flow rates.

### 3.3.4. Site-specific variables

For site-specific variables, we examined the geothermal gradient and the thermal conductivity of potential sites.

Ultimately, we compared the resulting  $R_b$  of all the cases we investigated and plot them as a scattered plot to indicate the range of variations that may result in performance differences between different CBHEs.

### 3.3.5. Geothermal gradient

The two non-design parameters, depth and thermal conductivity of the soil can also be examined, and provide some preliminary understanding of how the original CBHE would have experienced heat extraction when the CBHE is in a different location with different environmental parameters. Setting the geothermal gradient at 1 Kelvin per 100 meters and 5 Kelvin per 100 meters, the 100th hour's vertical temperature

distribution for the CBHE with original configuration except for being 1000 meters deep can be found in Figure 14.

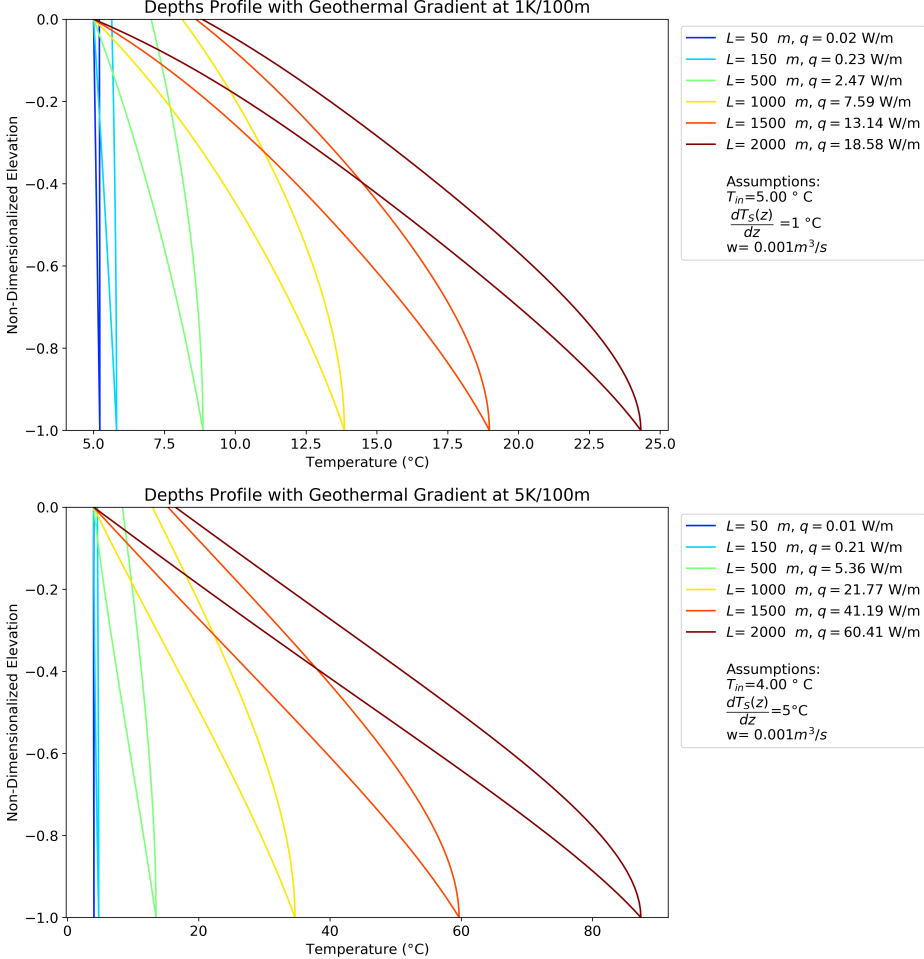


Figure 14: Vertical temperature distribution for the CBHE with original configuration for geothermal gradient of 1 Kelvin/100m (top) and 5 Kelvin/100m (bottom).

Similar to the discussion on the depths of CBHEs, deep CBHEs with large geothermal gradient produces the warmest temperatures at their bottom. Without proper insulation at the inner pipe and appropriate CBHE configuration, this thermal potential is difficult to recover for inadequately configured CBHE and flow rates. We're a geothermal gradient of 5 Kelvin per hundred meters, using the configuration already selected, the resulting temperature profile. As can be observed from Figure 15, the temperature out and the heat extraction rate are both much further improved for the deeper boreholes ( $L \geq 1000\text{m}$ ), while for shallower boreholes ( $L \leq 500\text{m}$ ), the benefit of insulating the inner pipe, increasing the pipe thickness or changing the flow rate did not create discernably visible differences. As the temperature at the outlet also exceeds  $30 \text{ }^{\circ}\text{C}$  for the deeper boreholes, it is possible to use CBHEs for direct heating, but potentially with additional upper insulation where the injected water regenerates the upper part of the CBHE. As can be observed from Figure 15, the temperature out and the heat extraction rate are both much further improved for the deeper boreholes ( $L \geq 1000\text{m}$ ), while for shallower boreholes ( $L \leq 500\text{m}$ ), the benefit of insulating the inner pipe, increasing the pipe thickness or changing the flow rate did not create discernably visible differences. As the temperature at the outlet also exceeds  $30 \text{ }^{\circ}\text{C}$  for the deeper boreholes, it is possible to

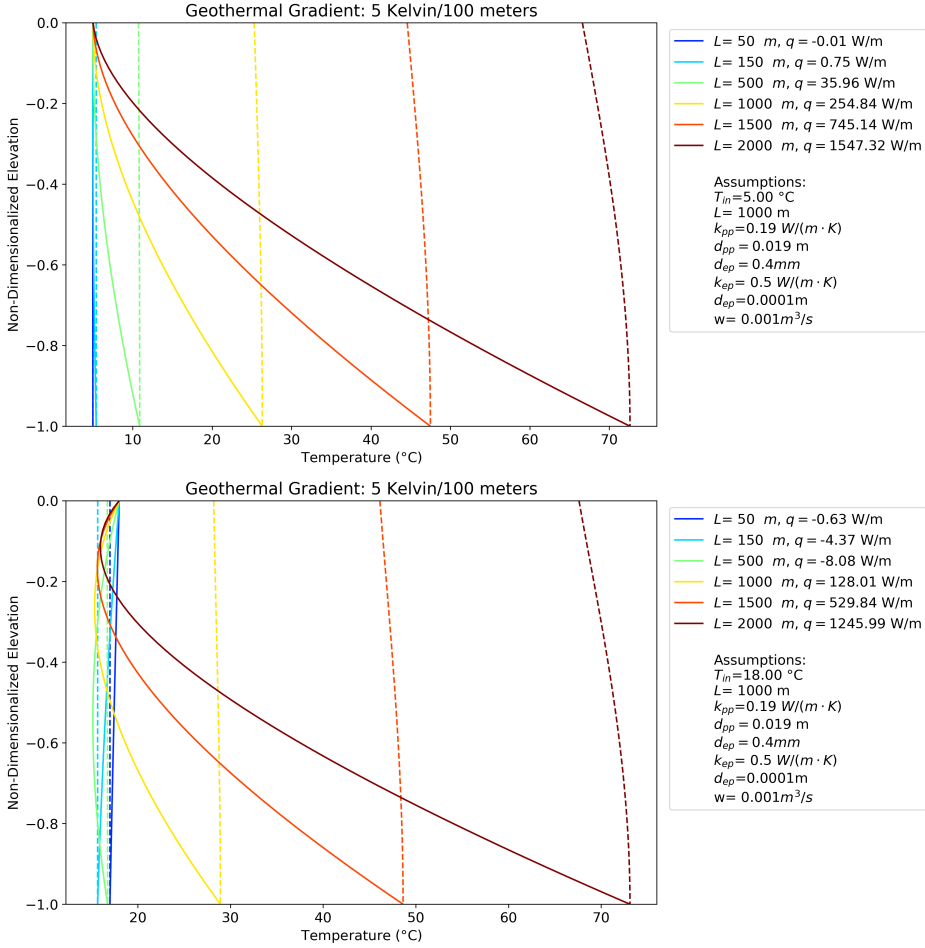


Figure 15: Vertical temperature distribution for the CBHE with original configuration for  $T_{in} = 5^{\circ}\text{C}$ (top) and  $T_{in} = 18^{\circ}\text{C}$  (bottom) with a geothermal gradient of 5 Kelvin per hundred meters.

use CBHEs for direct heating, but potentially with additional upper insulation where the injected water regenerates the upper part of the CBHE.

Similarly, for a geothermal gradient of 3 Kelvin per hundred meters, the temperature distribution inside the CBHE can be simulated at the 100th hour as Figure 16. The resulting temperature distribution inside the borehole shows, in general, a smaller heat extraction rate when the injection temperature is  $18^{\circ}\text{C}$  for boreholes that have a length  $L \geq 1000\text{m}$ . The direct heating potential appears to only be available for boreholes that are deeper than 1500m according to Figure 16 since the temperature out of  $L = 1000\text{m}$  drops to just  $12.4^{\circ}\text{C}$ .

Also examining the lowest geothermal gradient of 1 Kelvin per hundred meters, the temperature distribution inside the CBHE can be simulated at the 100th hour as Figure 17. Increasing the inlet temperature does not result in any improvement in heat extraction rate with any depth assigned. Injecting warmer water does appear to have effectively regenerated the borehole and can be seen as CBHEs being feasible for cooling when the geothermal gradient is smaller, or the well is shallower.

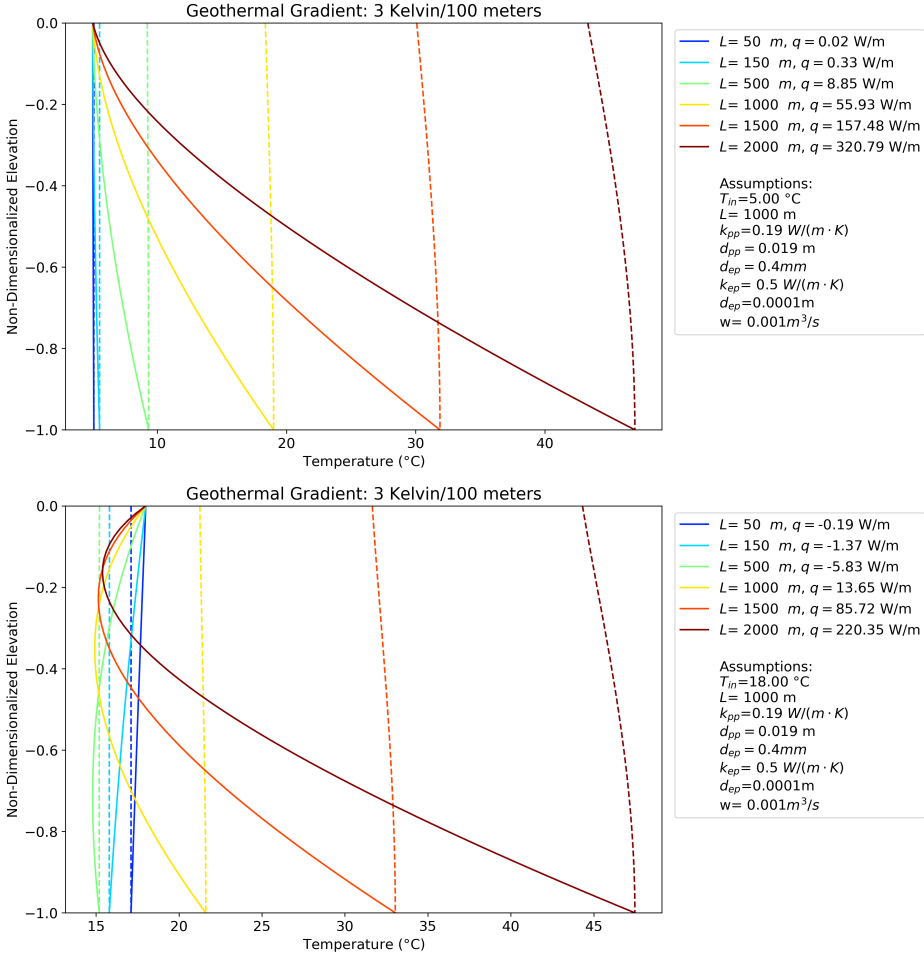


Figure 16: Vertical temperature distribution for the CBHE with original configuration for  $T_{in} = 5^{\circ}\text{C}$ (top) and  $T_{in} = 18^{\circ}\text{C}$  (bottom) with a geothermal gradient of 3 Kelvin per hundred meters.

### 3.3.6. Soil thermal conductivity

It is nearly impossible to determine the soil thermal conductivity before drilling and rigorous thermal response test (TRT), hence we only tested a specific range of possible thermal conductivity of soil, as shown in Figure 18. In this scenario, the rest of the borehole parameters were held constant to test for the temperature increase along the flow path to determine the influence of the soil conductivity on the progressive heat transfer. The thermal conductivity of the ground, on the other hand, is set to vary between 2.5 to 3.5  $\text{W}/(\text{m} \cdot \text{K})$ , which led to the following results in Figure 18 for a 1000m-deep borehole.

The larger the soil conductivity, the more substantial amount of heat absorbed from the downward flow through the annulus, and maintains warmer through the upward inner pipe, as can be expected with consistent inner pipe thermal conductivities. This small temperature increase is slightly diminished from the temperature gradient between the downward and upward flow as is shown in Figure 18, where the outlet temperatures exhibit a smaller separation when compared to the temperature separation at the bottom of the borehole.

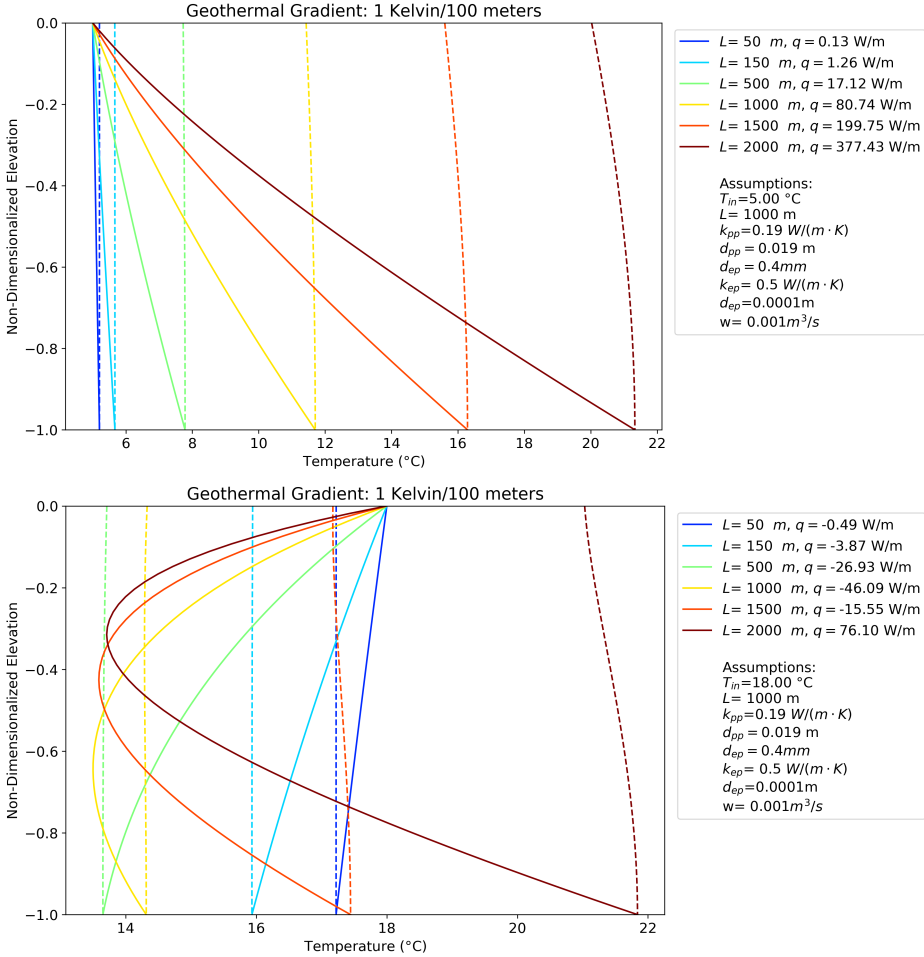


Figure 17: Vertical temperature distribution for the CBHE with original configuration for  $T_{in} = 5^{\circ}\text{C}$ (top) and  $T_{in} = 18^{\circ}\text{C}$  (bottom) with a geothermal gradient of 1 Kelvin per hundred meters.

### 3.3.7. Performance Implications

The temperature variation along the distance travelled for a random water particle can also be tracked via the vertical temperature profile calculation as shown in Figure 19 for a 1000m-deep CBHE with its key differences marked out in legends. The influence of our optimisation attempt was evident in the form of temperature at the outlet and heat extraction rate variation along the depth. The temperature lift through the entire CBHE defines the overall performance cap through Carnot efficiency. We found varying both the flow rate and the thickness of the inner pipe may lead to a central pipe condition that is close to lossless along the outlet channel, while the thermal conductivity of the pipe does not change the resulting heating potential significant. This graph does not capture the added complexity when depth also becomes a variable for optimisation. A multivariate analysis that utilises either Monte Carlo methods or other statistical approaches could be beneficial to determine the improvement of proposed design over one another instead of the results shown here in Figure 19.

By changing the configuration and/or thermal properties of a CBHE, it is possible to either have the heat exchange along the downward (annulus) pathway increased, resulting in raised bottom of borehole temperature, as is with the case of varying the soil thermal conductivity between  $2.5$  and  $3.5\text{ W}/(\text{m}\cdot\text{K})$ , or changing the thickness of the borehole wall to  $0.01\text{ m}$ . The latter also decreases the temperature along the

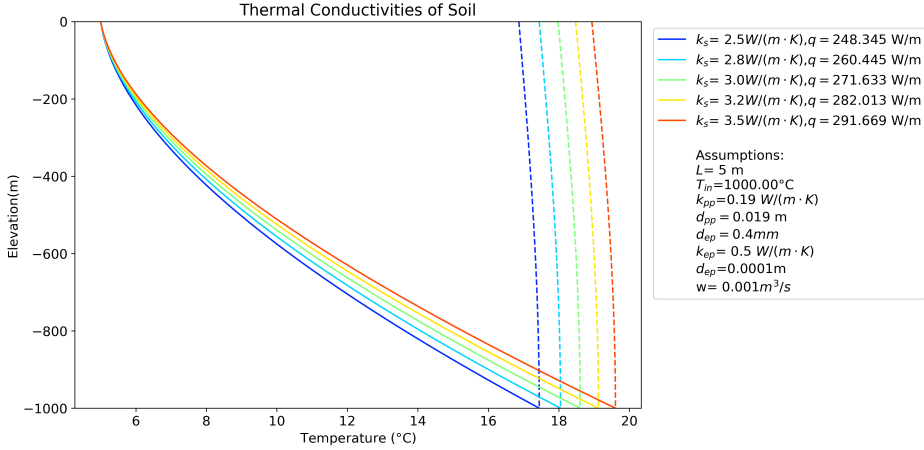


Figure 18: Influence of Soil Thermal Conductivity ( $k_s$ ) on the thermal performance

upward (inner pipe) pathway, which can be made possible by assigning an ideal thermal conductivity of an inner pipe at a thermal conductivity of  $k_{pp} = 0.007 \text{ W}/(\text{m}\cdot\text{K})$  which is difficult to implement in real projects as it was the thermal conductivity of vacuum-insulated steel pipes. As was pointed out in the discussion for varying the flow rate, however, an alternative to achieve maximised COP with a minimised geothermal depletion by using a significantly increased flow rate to produce turbulence flow inside the inner pipe to harvest the increased temperature at the bottom of the CBHE. The resulting COP from the CBHE will likely not only be a function of the temperature of water at the outlet, the flow rate, but also the amount of pumping power (operational cost) that went into ensuring the functioning of the overall system, which goes beyond the scope of this current paper. As was pointed out in the discussion for varying the flow rate, however, an alternative to achieve maximized COP with a minimized implication on geothermal depletion can also be achieved by using a significantly increased flow rate to achieve turbulence flow inside the inner pipe, so that the temperature increase at the bottom of the CBHE can be maintained at the outlet. The resulting COP from the CBHE will likely not only be a function of the temperature out, the flow rate, but also the amount of pumping power (operational cost) that went into ensuring the functioning of the overall system, which goes beyond the scope of this current paper.

#### 4. Discussion and Further Optimization

##### 4.1. Room for improvement

The proposed model, despite its relatively easier usage and customizability in contrast to existing libraries, has many constraints. A primary constraint is the lack of further customizability.

It's also important to stress that this model only applies to estimation of borehole resistance measured at the in-situ TRT tests for borehole heat exchangers. This means only nearly-constant-injection-rate heat injection is considered. In addition, the flow rate and the flow direction also do not vary in our solve solution. Although it is not very common to change the flow rate or flow direction inside a CBHE, we may need to operate a CBHE more flexibly to achieve desirable temperature distribution along the DTS cable installed inside the CBHE.

In order to achieve the temperature gradient as desirable as the one shown in the conceptual illustration in Figure 1, we need to optimize the temperature distribution and ultimately the temperature of the water coming back from the central tube. We believe it's important to also acknowledge the importance of an analytical model that might help model the real-time temperature distribution upon heat injection/extraction

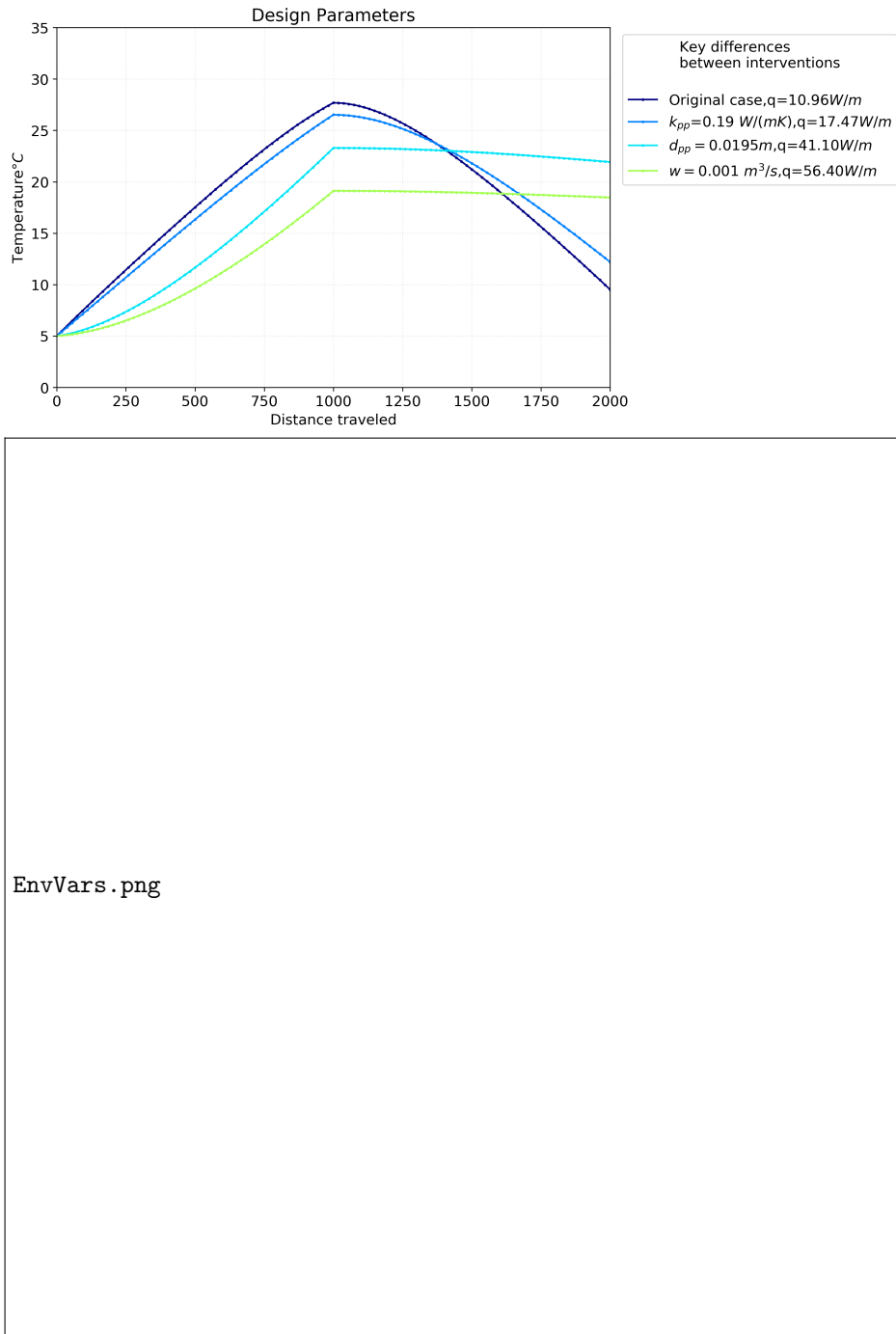


Figure 19: Temperatuer variation along distance traveled for different CBHE configurations for design variables (top) and environmental parameters (bottom),  $L = 1000\text{m}$ ,  $T_{in} = 5^\circ\text{C}$  and  $w = 0.058\text{m}^3/\text{s}$  as well as 30 Kelvin/km geothermal gradient before otherwise specified.

for potential model predictive control algorithms. And despite lack of existing methods that allows us to do so, a combined analytical and numerical solution that stores the temperature distribution of both the water and the soil temperature from the last time step may be developed in subsequent study to evaluate these potential improvement upon the existing approach the BHEs.

#### 4.2. Cost implications

It's also important to consider the cost implications of drilling deeper despite the potential geothermal gradient. Kavanaugh and Rafferty (2014) pointed out that the relationship between adding insulation and increasing the depth of borehole heat exchanger. In the meantime, the cost of drilling is also a factor that could impact the design of BHEs. As the cost of drilling could consist of over 50% of the overall cost when constructing new BHEs, it is crucial to understand the implications of suggesting drilling deeper and potentially larger borehole heat exchangers.

#### 4.3. Room for further investigations

- [1] E. Zanchini, S. Lazzari, A. Priarone, Improving the thermal performance of coaxial borehole heat exchangers, *Energy* 35 (2) (2010) 657–666.
- [2] L. Dijkshoorn, S. Speer, R. Pechnig, Measurements and Design Calculations for a Deep Coaxial Borehole Heat Exchanger in Aachen, Germany, *International Journal of Geophysics* 2013 (2013) 1–14.
- [3] M. Prandin, Exergy Analysis at the Community Level: Matching Supply and Demand of Heat and Electricity in Residential Buildings., Ph.D. thesis, Stockholm, Sweden (2010).
- [4] L. Rybach, W. J. Eugster, R. J. Hopkirk, B. Kaelin, Borehole heat exchangers: longterm operational characteristics of a decentral geothermal heating system, *Geothermics* 21 (5-6) (1992) 861–867.
- [5] J. E. ACUÑA, B. Palm, Experimental Comparison of Four Borehole Heat Exchangers, Copenhagen, 2008.
- [6] Ladislaus Rybach, Robert J. Hopkirk, Shallow and deep borehole heat exchangers - achievements and prospects, Florence, Italy, 1995.
- [7] H. Holmberg, J. Acuña, E. Næss, O. K. Sønju, Thermal evaluation of coaxial deep borehole heat exchangers, *Renewable Energy* 97 (2016) 65–76.
- [8] R. Beier, A. G. Ewbank, In-Situ Test Thermal Response Tests Interpretations, OG&E Ground Source Heat Exchange Study, Tech. rep. (Aug. 2012).  
URL [https://igshpa.org/wp-content/uploads/2019/06/In\\_situ\\_TRT\\_report.pdf](https://igshpa.org/wp-content/uploads/2019/06/In_situ_TRT_report.pdf)
- [9] W. Li, D. Sadigh, S. S. Sastry, S. A. Seshia, Synthesis for Human-in-the-Loop Control Systems, Lecture Notes in Computer Science, Springer Berlin Heidelberg, 2014, pp. 470–484.
- [10] F. GUILLAUME, Analysis of a novel pipe in pipe coaxial borehole heat exchanger, Ph.D. thesis, KTH Industrial Engineering and Manage, Stockholm, Sweden (2011).
- [11] J. Liu, F. Wang, W. Cai, Z. Wang, Q. Wei, J. Deng, Numerical study on the effects of design parameters on the heat transfer performance of coaxial deep borehole heat exchanger, *International Journal of Energy Research* doi:10.1002/er.4357.  
URL <https://onlinelibrary.wiley.com/doi/abs/10.1002/er.4357>
- [12] G. Shrestha, Y. Uchida, T. Ishihara, S. Kaneko, S. Kuronuma, Assessment of the Installation Potential of a Ground Source Heat Pump System Based on the Groundwater Condition in the Aizu Basin, Japan, *Energies* 11 (5) (2018) 1–14.  
URL <https://ideas.repec.org/a/gam/jenres/v11y2018i5p1178-d145058.html>
- [13] R. A. Beier, J. Acuña, P. Mogensen, B. Palm, Borehole resistance and vertical temperature profiles in coaxial borehole heat exchangers, *Applied Energy* 102 (C) (2013) 665–675.  
URL <https://ideas.repec.org/a/eee/appene/v102y2013icp665-675.html>
- [14] R. A. Beier, J. Acuña, P. Mogensen, B. Palm, Borehole resistance and vertical temperature profiles in coaxial borehole heat exchangers, *Applied Energy* 102 (2013) 665 – 675.
- [15] American Society of Heating, Refrigerating and Air-Conditioning Engineers, 2013 Ashrae Handbook: Fundamentals, inch-pound ed. Edition, Atlanta, Ga.: Ashrae, 2013.
- [16] L. R. Ingwersoll, O. J. Zobel, A. C. Ingwersoll, Heat conduction with engineering, and other applications, *Physics Today* 8 (3) (1955) 17–17.
- [17] S. P. Kavanaugh, Simulation and Experimental Verification of Vertical Ground-coupled Heat Pump Systems.